Received: 20 May 2022 | Revised: 6 September 2022 | Accepted: 21 September 2022

DOI: 10.1002/hyp.14716

RESEARCH ARTICLE

WILEY

Understanding the hydrological regime based on the runoff events in a mountainous catchment with seasonally frozen soil in the Qinghai-Tibet plateau

Pengfei Lin | Zhibin He | Jun Du | Longfei Chen | Xi Zhu | Quanyan Tian

Linze Inland River Basin Research Station, Chinese Ecosystem Research Network, Key Laboratory of Eco-hydrology of Inland River Basin, Northwest Institute of Eco-Environment and Resources, Chinese Academy of Sciences, Lanzhou, China

Correspondence
Zhibin He, Linze Inland River Basin Research Station, Chinese Ecosystem Research Network, Key Laboratory of Eco-hydrology of Inland River Basin, Northwest Institute of Eco-Environment and Resources, Chinese Academy of Sciences, Lanzhou 730000, China.
Email: hzbmail@lzb.ac.cn

Funding information
National Natural Science Foundation of China, Grant/Award Numbers: 41901044, 41901050, 41621001; The Strategic Priority Research Program of the Chinese Academy of Sciences, Grant/Award Number: XDA23060301; Foundation for Excellent Youth Scholars of Northwest Institute of Eco-Environment and Resources, Chinese Academy of Sciences, Grant/Award Number: FEYS2019019

Abstract

Seasonal thawing of frozen soil will significantly affect the hydrological regime, water storage capacity and ecosystem services in the future, which contributes to the uncertainty of regional water resources. However, based on the scale of runoff events, the mechanism of seasonal frozen soil thawing on the hydrological regime are still unclear. In this study, we systematically analysed the runoff characteristics and interactive effects of environmental factors and pre-event catchment state on runoff processes based on the runoff event scale, using data sets of air temperature, precipitation, runoff, soil moisture, and soil temperature observed in a mountainous catchment with seasonally frozen soil distribution on the Qinghai-Tibet Plateau from 2010 to 2019. It was found that the event runoff coefficient did not increase significantly with the increase of precipitation. Event runoff coefficients exhibited strong seasonality. The catchment exhibited a gradual increase in the event runoff coefficient with increasing pre-event baseflow and antecedent soil moisture, especially during stable period (August to November). Event runoff generation through infiltration excess as the result of intensive rainfall seemed to be only possible in the stable period, while heavy precipitation events were common during this period. Normalized event peak discharge and event runoff coefficient showed positive trends with changes in pre-event catchment state indicators, which were commonly observed phenomena in runoff events. For this catchment, the increased storage capacity pre-event saturation may be the main mechanism of event runoff generation, as it was unlikely that a single precipitation event would lead to catchment saturation. Soil temperature affects runoff processes through both direct effects on runoff processes and indirect effects on pre-event catchment state. Temperature indicators were the most important predictors of runoff changes in the Qinghai-Tibet Plateau.

KEYWORDS
hydrological regime, Qinghai-Tibet plateau, runoff events, seasonally frozen soil

1 | INTRODUCTION

In recent decades, the hydrological cycle and hydrogeology of high latitudes and high altitudes have undergone significant changes due to climate change effects, such as glacial retreat, melting snow, and permafrost degradation. These changes will significantly affect runoff, hydrological regime, seasonal distribution, water storage capacity and ecosystem services in the future, which contribute to the uncertainty of regional water resources.

A rise in temperatures may lead to a decrease in permafrost distribution in alpine catchment in the coming decades (Teufel & Sushama, 2019; Jin et al., 2021). A significant amount of permafrost degradation alters soil water storage and weathered sediment storage. Steep topography and the release of large amounts of weathered sediments lead to changes in water storage behaviour, in addition, permafrost degradation in this environment may affect water storage capacity and subsurface flow paths, affecting the catchment runoff response (Koch et al., 2014; Lafrenière & Lamoureux, 2019). Taking trends of climate change projections into consideration, understanding the impact of climate change on runoff behaviour in permafrost distributed within basins is critical for regional water resource forecasting and management.

The low relative permeability of frozen soils has been widely recognized as a potentially import driver for partitioning snowmelt between runoff, shallow interflow, or deep groundwater flow paths(Ireson et al., 2013; Rey et al., 2021). When frozen, the effective permeability and infiltration capacity of soil are diminished, as pore ice inhibits water movement through the subsurface (Rey et al., 2021; Watanabe & Osada, 2011). Numerous studies (Han & Menzel, 2022; Lafrenière & Lamoureux, 2019; Lin, Gao, et al., 2020; Shi et al., 2020), analysed impacts of permafrost degradation on runoff response. The results indicated that permafrost-rich catchments had rapid runoff responses dominated by near-surface drainage and larger event runoff coefficients, while seasonal runoff variability was reduced. However, permafrost degradation can be divided into the increase of the permafrost active layer, and the thawing of seasonal frozen soil, which have different hydrological process characteristics due to their different frost heave and thaw subsidence processes (Shi et al., 2020; Teufel & Sushama, 2019). Seasonal freeze–thaw primarily affects near-surface areas by increasing the water storage capacity within the soil and reducing the ability of water to infiltrate the soil surface. These changes result in greater baseflow, deeper flow paths that often connect near-surface, and deeper aquifers (Smith et al., 2019; Steelman et al., 2010). The differences in the hydrological characteristics of these frozen soils creates uncertainty in the study of watershed hydrological processes.

Qilian Mountains, on the northern edge of the Qinghai-Tibet Plateau, are representative of the mountains in the arid region of China, and the headwaters of the three major inland rivers in the Hexi Corridor. It plays an important role in water conservation, biodiversity protection, and maintaining ecological balance (Cheng et al., 2014; Sun et al., 2016). The Qilian Mountains are one of the most sensitive regions to global climate change. In recent years, temperature, precipitation and extreme climate events in the Qilian Mountains have increased with global climate change (Lin et al., 2018). These climate-sensitive results are directly reflected in the dramatic increase in runoff in inland river basins, the retreat of permafrost to higher altitudes, expansion of seasonally frozen ground, and the significant increase in runoff during the freezing season (November to March)(Qin et al., 2016). As the source of rivers, water storage capacity and the process of production and confluence have changed caused by the degradation of permafrost in the high mountains of the Qilian Mountains play an important role in water conservation and water resource regulation functions of the entire mountain basin. Although scholars have carried out related research on the permafrost hydrological process in the Qinghai-Tibet Plateau, they mostly focused on the impact of increased permafrost active layer on runoff, and large-scale and macroscopic simulation research (Gao et al., 2021; Ma et al., 2017). There are few studies that examine the impact of seasonal frozen soil on runoff characteristics, particularly from the perspective of runoff events. Simultaneously, the comprehensive observation and acquisition of runoff event scale data is a challenge for the study of hydrological process of seasonally frozen soil in alpine mountains owing to the limitations of the natural environment and traffic conditions. There is a lack of knowledge about the hydrological processes of seasonal frozen soil in the Qinghai-Tibet Plateau at slope to watershed scales as a result of these factors.

Hillside hydrological responses are often nonlinear and therefore difficult to assess and predict directly. As the basic unit of the runoff process, runoff event is the most effective medium to study the hillside runoff process and its influencing factors. Therefore, this study aims to identify the runoff process, seasonal distribution changes and their respective controlling factors in seasonally frozen soil distributed in mountain basins, from the perspective of runoff events, which provide a different understanding of the hydrological processes of mountain permafrost in the Qinghai-Tibet Plateau.

2 | STUDY AREA AND DATA

2.1 | Study area

The research site was in the Pailugou catchment (100°17′ E, 38°24′N) of the Qilian Mountains on the northern edge of the Qinghai-Tibet Plateau (Figure 1). The catchment's total area was 2.93 km^2, and elevation ranged from 2700 to 3860 m. Seasonally frozen soils were widespread at middle and high elevations (2900–3860 m). The bedrock was mainly calcareous rock, covered with a relatively thin soil layer. Soils had a coarse texture, intermediate organic matter content, and *pH* ranging between 7 and 8. Owing to large temperature and precipitation gradients, vegetation formed a mosaic of grassland, scrubland, and forest.

2.2 | Data

2.2.1 | Meteorological measurements

Meteorological elements such as air temperature, precipitation, wind velocity, radiation etc., were recorded by IMKO ENVIS environmental measurement system which was installed at an elevation of 2700 m, and meteorological observation system (Campbell Scientific, Inc.) at 2800 and 3200 m since 2002, to continually monitor microclimate in the catchment at 30 min intervals. Additionally, air temperature and precipitation were measured and recorded with an automatic sensor (RG50, SEBA Hydrometrie, Germany) at elevations of 2600–3800 m

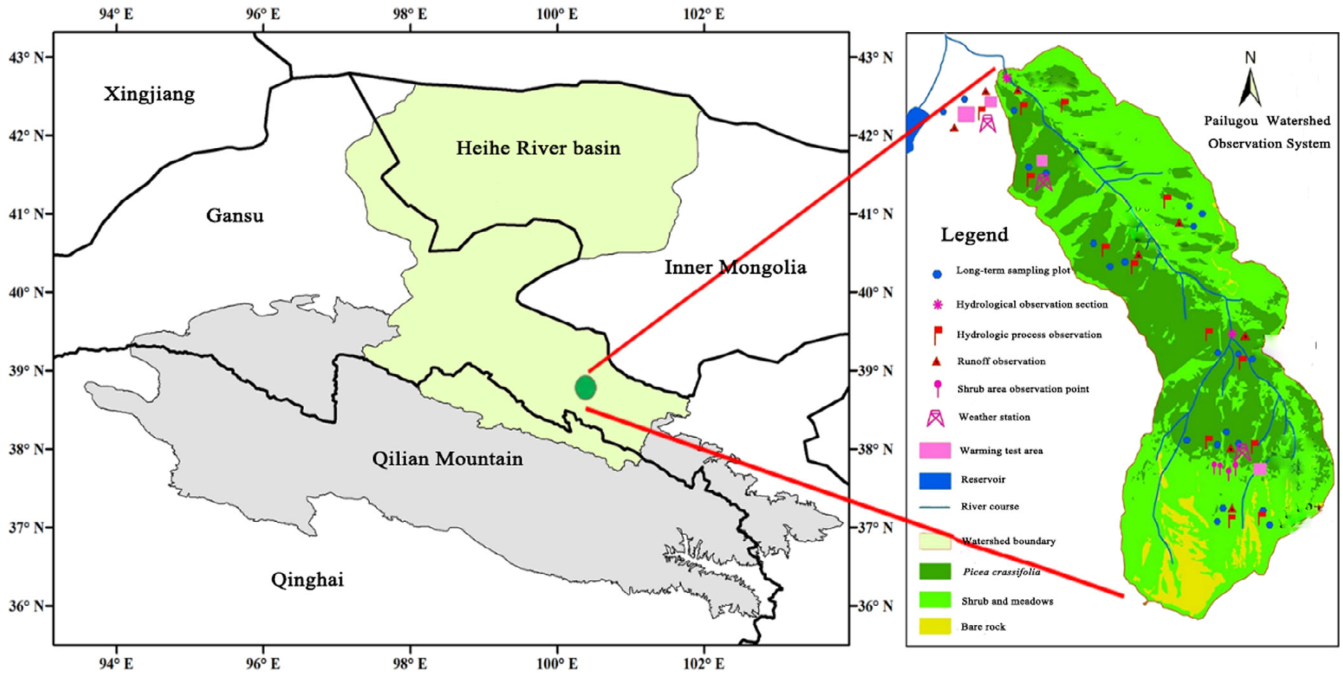

FIGURE 1 Study area and observation instrument position

at 200 m intervals for a total of 14 observation points from 2010 to 2019.

2.2.2 | Runoff measurements

The catchment runoff volume was measured in a weir installed at 2650 m elevation, downstream from the study area. The runoff volumes were recorded automatically using a water level gauge (SW40, China) from 2002 to 2019. During cold season (December to March), part of the weir would freeze resulting in the meters not functioning owing to an insufficient volume of runoff. Runoff volume was then measured using a container (volume $= 0.01778$ m^3). Each day, the time (seconds) taken for runoff to fill the container was measured, and then linear interpolation of runoff volumes was used between pairs of measurements to graph, the results, and calculate total runoff during this period (the entire winter).

2.2.3 | Soil moisture, temperature and soil freeze–thaw measurements

Volumetric soil water content and soil temperature were measured using ECH$_2$O (Decagon, Inc. Decagon, 140 USA) at depths of 5, 10, 20, 40, and 60 cm. The observation data was automatically collected and recorded by the EM50 series data collection system at 30 min intervals. Since 2008, three sets of ECH$_2$O were installed in the 2700, 2750, 2850, 3200, and 3400 m. To calibrate the ECH$_2$O data, soil moisture was measured using the oven-drying method (108°C) once every month during the growing season.

A set of permafrost apparatus ($n = 14$) was installed to monitor soil freezing and thawing. First, soil was excavated to a depth of 250 cm. To instal, the outer tube (jacket pipe) with a length of 300 cm and a diameter of 5 cm is pushed to soil depth of 250 cm. Simultaneously, a rubber freezing pipe, with a length of 250 cm and a diameter of 1 cm, was filled with water. The gap between the jacket pipe and the soil was then backfilled to prevent precipitation from entering. The thickness of frozen soil was measured on a scale in the rubber freezing pipe that shows frozen water column depth.

3 | METHODS

3.1 | Baseflow separation

In accordance to previous research (Lin, He, et al., 2020), the recursive digital filter (RDF) was used for baseflow separation in this study. The filter equation is as follows (Lyne & Hollick, 1979):

$$q_t = \alpha q_{t-1} + \frac{1+\alpha}{2}(Q_t - Q_{t-1}). \tag{1}$$

where q_t is filtered streamflow at time step t, Q_t is total streamflow, and α is the filter parameter. Then the filtered baseflow is obtained as

$$b_t = Q_t - q_t. \tag{2}$$

The filter parameter α in Equation (1) is determined from previous published data and results located in the same area (Chen et al., 2014; Lin, He, et al., 2020). Therefore, the filter parameter α was taken as

TABLE 1 Event characteristics and indicators of pre-event catchment state used in this study, modified from Tarasova et al. (2018)

Characteristics	Description	Abbreviation	Unit
Event runoff coefficient	Ratio between the volumes of quick runoff (mm) and the attributed rainfall and snowmelt events (mm)	R_c	dimensionless
Event time scale	Ratio between quick runoff volume (mm) and peak discharge (mm/day)	T_s	days
Event rise time	Duration (day) from the beginning of the event till the day when peak discharge was observed, normalized by the total duration (day) of the event	R_t	dimensionless
Normalized event peak discharge	Maximum event flow normalized (mm/d) by the long-term average flow (Q50, mm/d)	P_e	dimensionless
Volume of precipitation	Sum of precipitation volumes (mm) contributing to a certain runoff event	P_{vol}	mm
Antecedent soil moisture	Catchment average of the water content (m^3/m^3) within the entire soil column in the 7 days preceding the event	S_{am}	m^3/m^3
Pre-event baseflow	Baseflow (mm/day) in the day preceding the runoff event	Q_{base}	mm/day
0–60 cm soil temperature	The average value of soil temperature content is in the soil layer 0–60 cm	ST_{0-60}	°C
0–60 cm soil moisture	The average value of soil moisture content (m^3/m^3) is in the soil layer 0–60 cm	Sm_{0-60}	m^3/m^3
Pre-event catchment state	Comprehensive index of catchment status	*PCS*	dimensionless

0.98 considering the average relative error of Baseflow index (BFI) in this study. The time series was filtered three times: forward, backward, and forward again.

3.2 | Identification of runoff events

The streamflow time series were screened to identify runoff events after the separation of baseflow, which are characterized by the appearance of peaks, beginning times, and end times (Mei & Anagnostou, 2015; Tarasova et al., 2018). A peak occurs at day *i* if $Q_i > Q_{i+1}$ and $Q_i > Q_{i-1}$. The event begins at the time before the peak occurs, when the total runoff equals the baseflow before the peak occurs. However, it ends as soon as runoff has drop to the baseflow again. The minimal duration of a runoff events were set to one day due to the daily temporal resolution of the available time series. Finally, runoff events with only one peak were aggregated into a reference group of single-peak events, the rest classified as multi-peak events. The detailed identification method is shown in Tarasova et al. (2018) (Table 1).

3.3 | Determining the drivers of rainfall-runoff events

Structural equation modelling were developed to explore relations between precipitation, temperature indicators and the pre-event catchment state effects on runoff events' processes. Four models were developed with the lavaan package version 0.6–9 (Rosseel, 2012) in R version 4.1.2: single-peak, multiple-peak, soil melting period, and stable

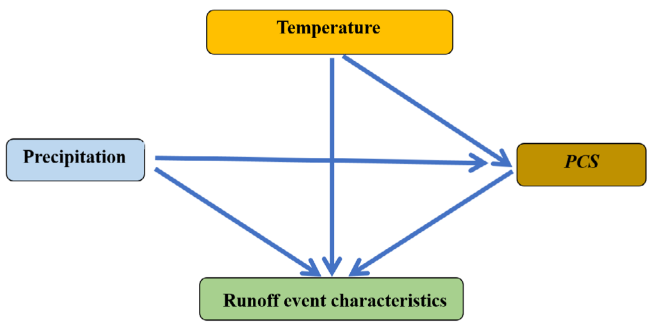

FIGURE 2 Conceptual causal model linking precipitation, temperature indicators and pre-event catchment state to runoff events through direct and indirect links

period models (R Core Team, 2019). The developed SEMs were based on the conceptual causal model outline in Figure 2. Daily average temperature, daily minimum temperature, and 0–60 cm soil temperature were modelled as direct effects on the runoff events processes and indirect effects on *PCS*. The indirect effect of temperature on runoff event is mainly reflected in the process of soil freezing and thawing. When frozen, the effective permeability and infiltration capacity of soil are diminished, as pore ice inhibits water movement through the subsurface. Q_{base} and Sm_{0-60} were used for the *PCS* variable and were modelled as direct effects on runoff events processes. Process of saturation excess runoff in the catchment are directly affected by antecedent soil moisture and baseflow. A runoff event occurs when precipitation infiltration fills soil pores, which increases soil moisture and baseflow until the threshold is reached. A natural log transformation was applied to the variables. For this study, fit was assessed through (1) comparative

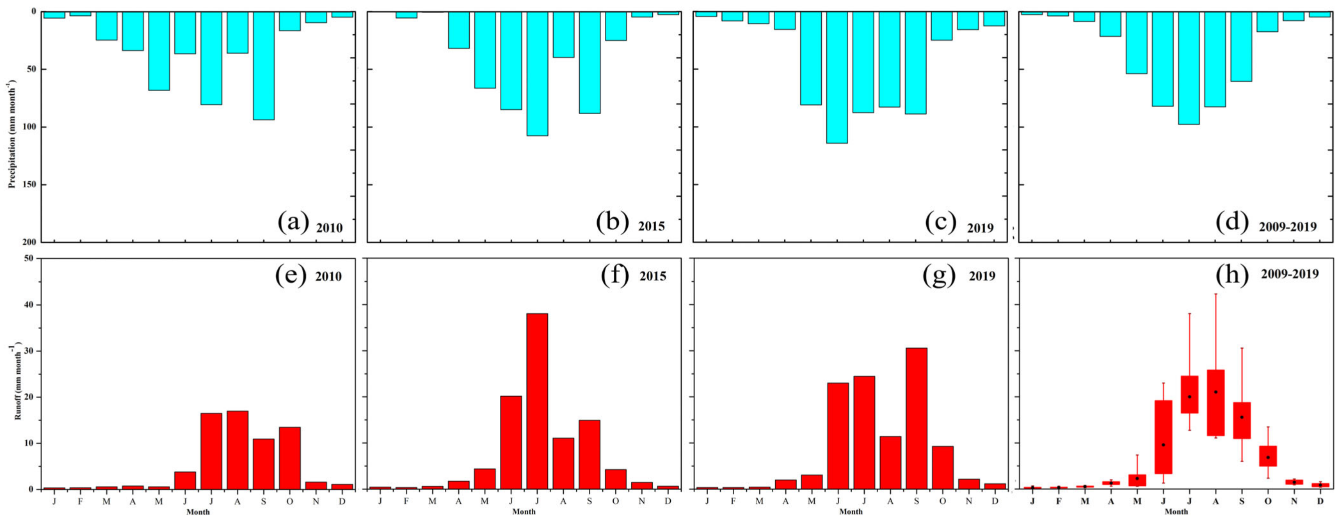

FIGURE 3 Precipitation and runoff characteristics of the catchment

fit index (cfi), which compared the fit of the target model to a null model, (2) root-mean-square error of approximation (RMSEA, $\alpha = 0.05$), which estimated data fit to the causal hypothesis, and (3) R^2 values indicated the percent of the variability in the dependent variables that the predictor variables explained.

4 | RESULTS

4.1 | Long-term runoff statistics for the catchment

The average precipitation and runoff were 442.9 and 80.0 mm respectively from 2010 to 2019 (Figure 3). Surface runoff was mostly generated during heavy rainstorms due to its high vegetation coverage. In addition, soil water, seepage, and groundwater were frequently exchanged in the catchment, due to the steep undifferentiated rock layer. Precipitation and runoff were concentrated in June to October, accounting for 80%–90% of the annual, respectively. The runoff in the remaining time was mainly interflow and baseflow.

In the absence of the true baseflow as a reference for comparison, baseflow separation was an important way to clearly identify the beginning of potential runoff events for studying hydrological regime in catchments. The RDF method was used to study the hydrological regime of the catchment from 2010 to 2019 and found that the average baseflow was 41.7 mm, and the BFI was 0.5217 with a range of 0.4515–0.5611 (Figure 4).

4.2 | Runoff event characteristics

4.2.1 | Variability of runoff event characteristics

The method developed by Tarasova et al. (2018) was used to identify runoff events. A total of 211 events were identified from a daily series of streamflow observations in the catchment from 2010 to 2019. Of these, 30.81% events were classified as multiple peak events.

Typical event variability of runoff event characteristics within the catchment is presented in Figure 5, where event characteristics (i.e., normalized peak discharge, runoff coefficient, rise time, and time scale) are plotted against several precipitation and pre-event catchment state indicators (i.e., antecedent soil moisture, pre-event baseflow, and soil temperature).

The normalized event peak discharge was closely related to precipitation characteristics and pre-event catchment state indicators, in single or multiple-peak events (Figure 5). The P_e increased proportionally to the volume of precipitation and pre-event baseflow in the catchment. However, the precipitation corresponding to the single-peak runoff events did not exceed 80.0 mm, and the pre-event baseflow was also less than 0.8 mm/day.

Figure 5 distinctly portrays a nonlinear relation between the event runoff coefficient and antecedent soil moisture, event runoff coefficient and soil temperature, peak discharge and antecedent soil moisture, and the peak discharge and soil temperature. Interestingly, multiple-peak events (grey dots in Figure 5), albeit exhibiting a similar trend to single-peak events (blue dots in Figure 5), showed obvious threshold behaviours in the occurrence conditions of the two events. For the multiple-peak events, distribution of precipitation with 0–137.0 mm, the antecedent soil moisture in all events was greater than 0.1 m^3/m^3, and the soil temperature is greater than 0°C. A phenomenon worth considering is that there was no obvious relationship between P_{vol} and R_c. No clear relation was also observed between event rise time and P_{vol} and *PCS*. The Q_{base} was only slightly affected the event time scale, R_c, and R_t, while it was a strong linear predictor of the P_e.

4.2.2 | Seasonal variation in runoff event characteristics

Based on previous studies (Yang et al., 2017), the dynamics of soil moisture in the catchment can be separated into soil melting period (April to July), stable period (August to November), soil freezing period

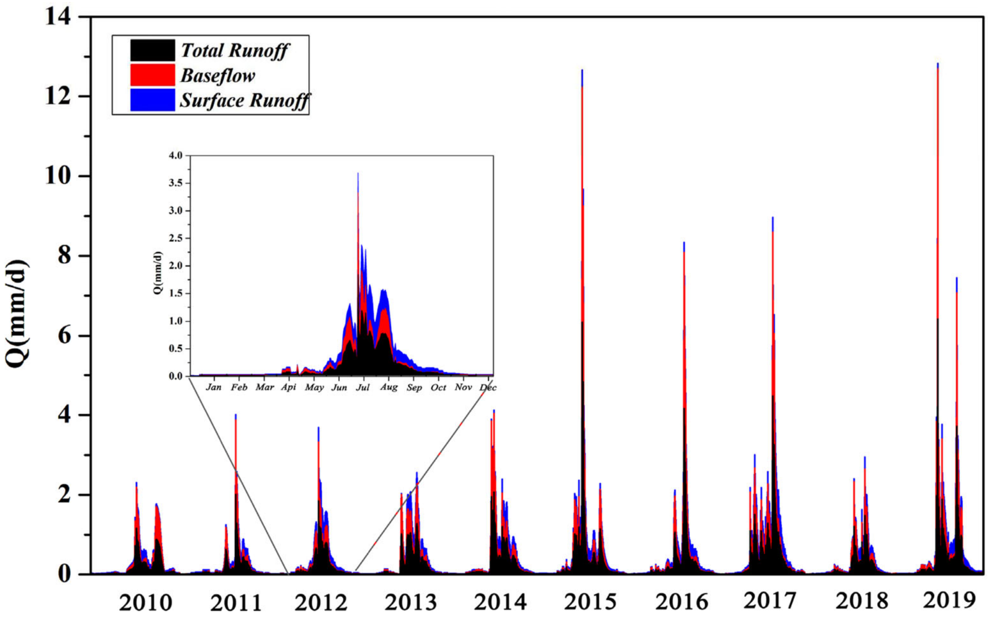

FIGURE 4 Characteristics of runoff components

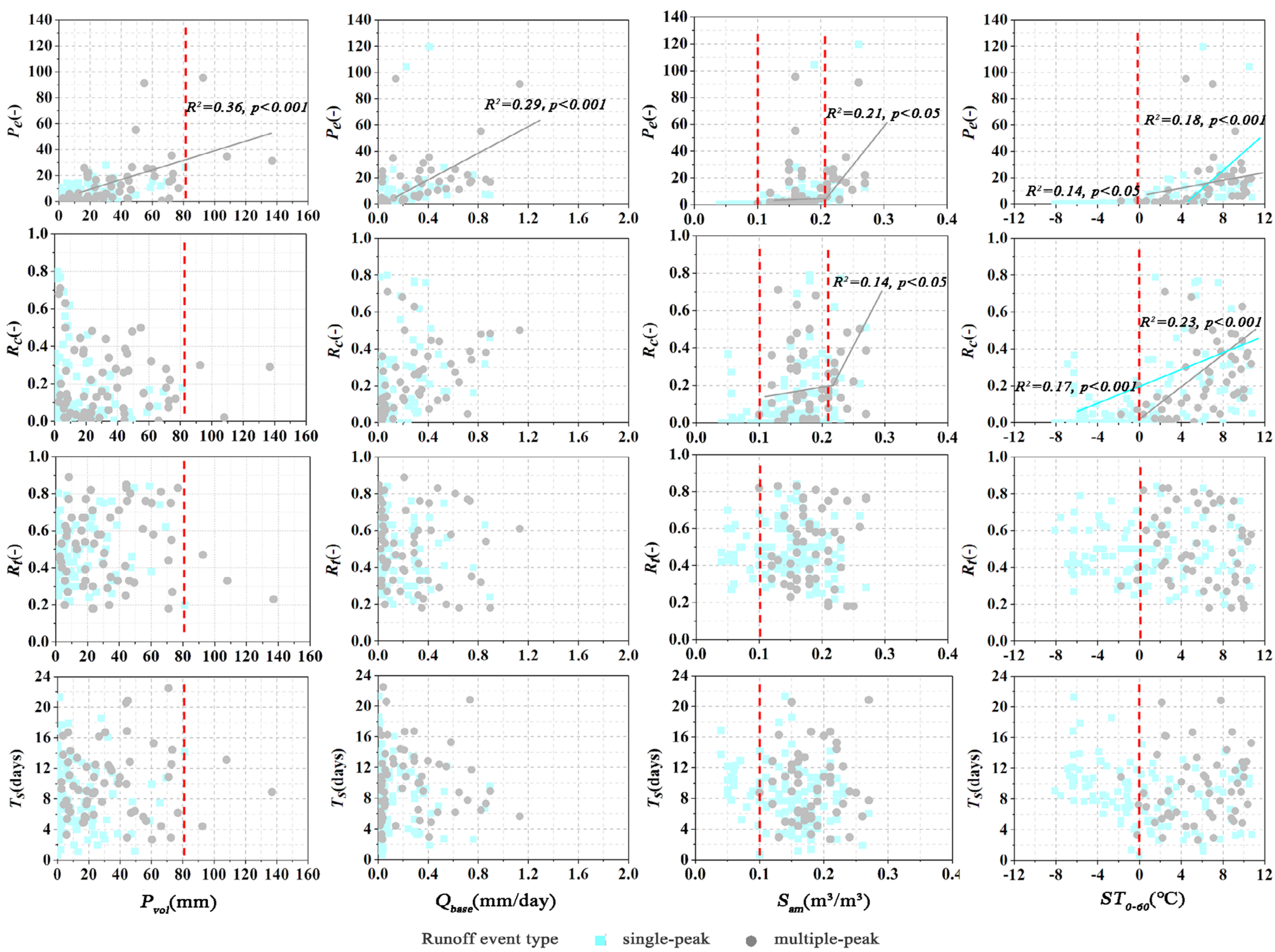

FIGURE 5 Relationship between runoff event characteristics and the indicators of pre-event catchment state

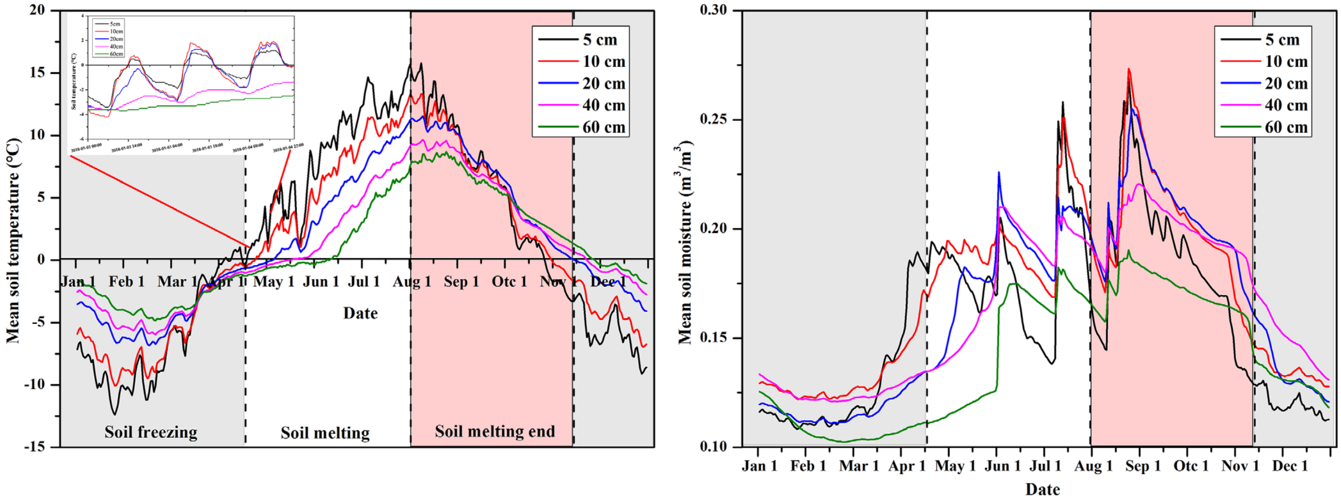

FIGURE 6 Mean daily soil temperature and moisture at 5, 10, 20, 40 and 60 cm depth in the study catchment, (a) soil temperature, (b) soil moisture

(December to March). Therefore, the hydrological regime was analysed in sections following the dynamics of soil moisture (Figures 6, 7, A1 and A2).

Runoff event characteristics had distinct differential over the three time periods. The hydrological regime in the catchment became complex, with seasonally frozen soil melting due to elevated soil temperatures in April to November. The soil moisture and runoff in the catchment showed a normal distribution consistent with the soil temperature. The soil temperature rose from 0 to 15°C (Figure 6) and we can clearly see an interesting phenomenon that the soil temperature of 0–20 cm layer is greater than 0°C from 10:00 to 21:00, and the soil temperature is less than 0°C from 21:00 to 9:00, which resulted in melting by day and freezing at night during the soil melting period. Multiple-peak events were mainly concentrated in the soil melting period, and stable period. The characteristics of multiple-peak events during these two periods were highly consistent with the overall multiple-peak events. Precipitation and melted snow cannot be completely converted into soil water and runoff, this results in an event rise time greater than the stable period and the normalized peak discharge, event runoff coefficient and event time scale less than the stable period, followed the pattern of melted snow contribution and soil moisture in single or multiple-peak events. Owing to the joint action of precipitation and seasonal permafrost melting, soil water moved, resulting in a reduction of shallow soil water, and surface runoff showed a rapid rise from August to November. The normalized peak discharge, event runoff coefficient, event rise time, and pre-event baseflow all reached the maximum state throughout the year. The effect of soil temperature on the characteristics of seasonal runoff events was more significant, and the characteristics of runoff events gradually increased with the increase of soil temperature during the soil melting period. As the soil temperature of the soil freezing period was −3.17°C, most of the water (precipitation, soil moisture, river stream) existed in a solid-state, and there was no significant change in the hydrological regime characteristics.

4.3 | Dynamics of response to runoff events

The results of the SEM revealed that temperature indicators control the hydrological regime in a catchment with seasonal frozen soil in semiarid mountains (Figure 8). The single-peak model explained 73% of the variance of runoff event characteristics (Figure 8a), whereas 52% of the variance in runoff event characteristics was explained by the multiple-peak model (Figure 8b). In the single-peak model, temperature indicators, which consisted of average temperature, lowest temperature and 0–60 cm soil temperature, had a strong direct positive effect on *PCS* and runoff event characteristics. Whereas precipitation had no significant negative influence on runoff event characteristics (Figure 8a). The *PSC*, which consisted of pre-event baseflow and 0–60 cm soil moisture, was strongly positively affected by the temperature indicators and not significantly negatively affected by precipitation. Finally, a strong positive effect was used jointly for the runoff event characteristics (Figure 8a). However, in the multiple-peak model, in addition to a strong positive effect of temperature indicators on *PCS*, there was no significant negative effect on runoff event characteristics. Precipitation had a minor positive effect on *PCS* and runoff event characteristics. The *PCS* was consistent with the single-peak model, with a strong positive effect on runoff event characteristics (Figure 8b).

Structural equation modelling results showed that runoff event characteristics consisted of single and multiple-peak, showing different driving mechanisms, which also had different driving factors in different seasons (Figures 8 and 9). A structural equation model was constructed based on seasonal characteristics to analyse the direct and indirect drivers of runoff event characteristics. The positive effect of the temperature indicators on the hydrological regime peaked in

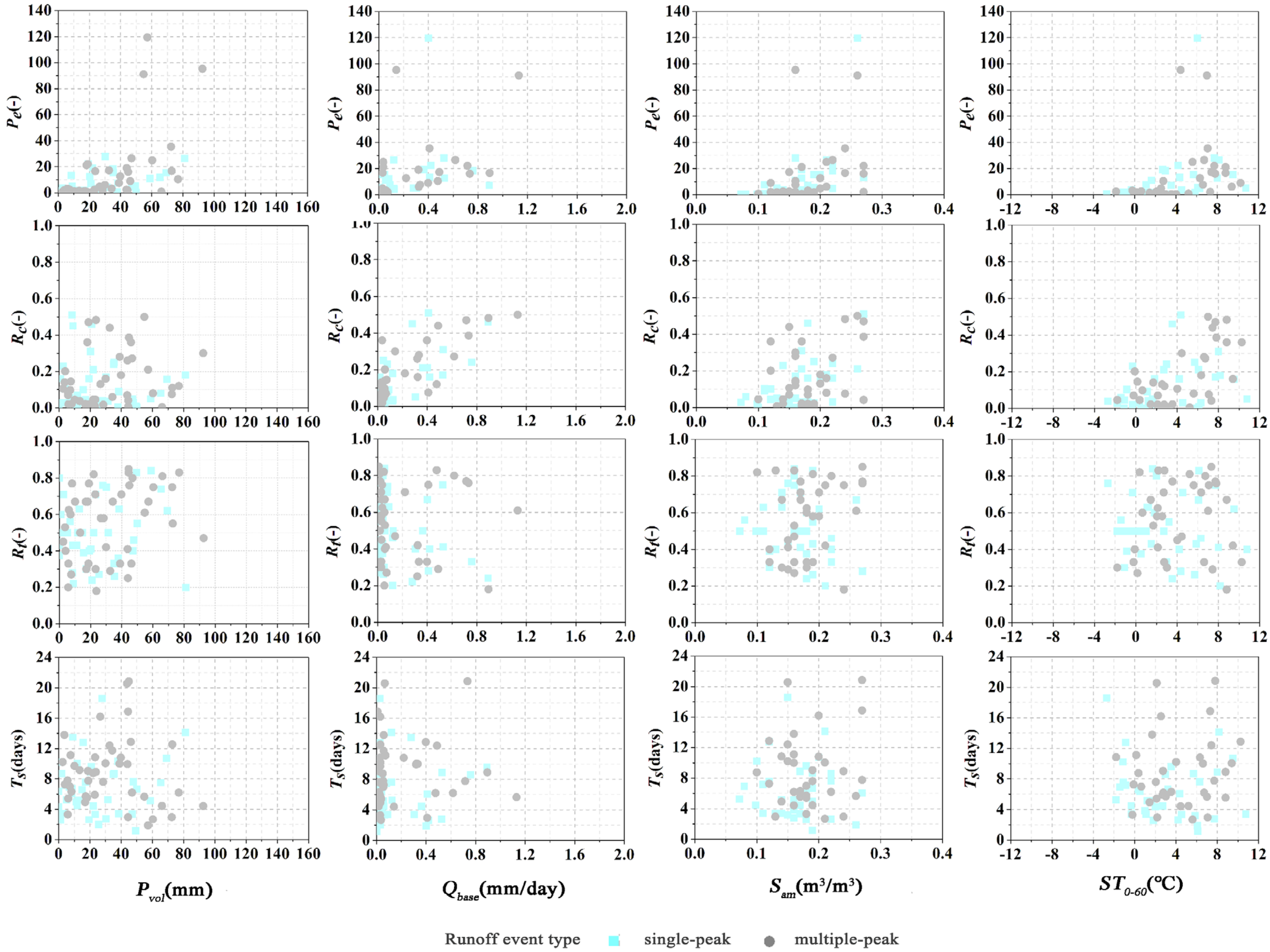

FIGURE 7 Seasonality of runoff event characteristics, soil melting period, April to July (stable period, August to November see in Figure A1, soil freezing period, November to April see in Figure A2)

the soil melting period. The characteristics of runoff events in this period were mainly determined by the temperature indicators, and precipitation had a slight no significant effect. In the stable period, the effects of precipitation and temperature indicators on runoff event characteristics were comparable, however, in different directions. The hydrological regime during the soil freezing period did not change significantly, and the runoff events were dominated by pre-event baseflow. Therefore, there was no structural equation model constructed based on the soil freezing period.

5 | DISCUSSION

5.1 | Particularity and universality of runoff events

Hillside hydrological responses are often nonlinear and therefore, difficult to assess and predict directly (Kirkby, 1988). As the basic unit of the runoff process, the runoff event was the most basic and effective medium to study the hillside runoff process and its influencing factors. Differences in runoff characteristics between single and multiple-peak events indicated differences in the mechanisms of runoff generation in different environmental conditions and seasons. The study of the event-to-event variability of runoff event characteristics during this period unveiled the existence of different runoff generation mechanisms in the mountains of arid regions. The findings suggest a complex interplay exists between changes in volume of precipitation events contribution, soil moisture, pre-event baseflow, and soil temperature. In arid mountain catchments, where storage capacity was high and infiltration excess or event-fed saturation dominates, a more pronounced influence of precipitation volume change of the event characteristics was noticeable in summer seasons.

Previous studies have regarded heavy precipitation as an important driving factor for the catchment runoff response (Edokpa et al., 2022; Huo et al., 2021; Rushlow & Godsey, 2017; Serrano-Notivoli et al., 2022); however, in this study, we found that the event runoff coefficient did not increase significantly with increased precipitation. This phenomenon is due to poorly developed soils in the alpine mountains and widespread rock fragments layers, which leads to leads

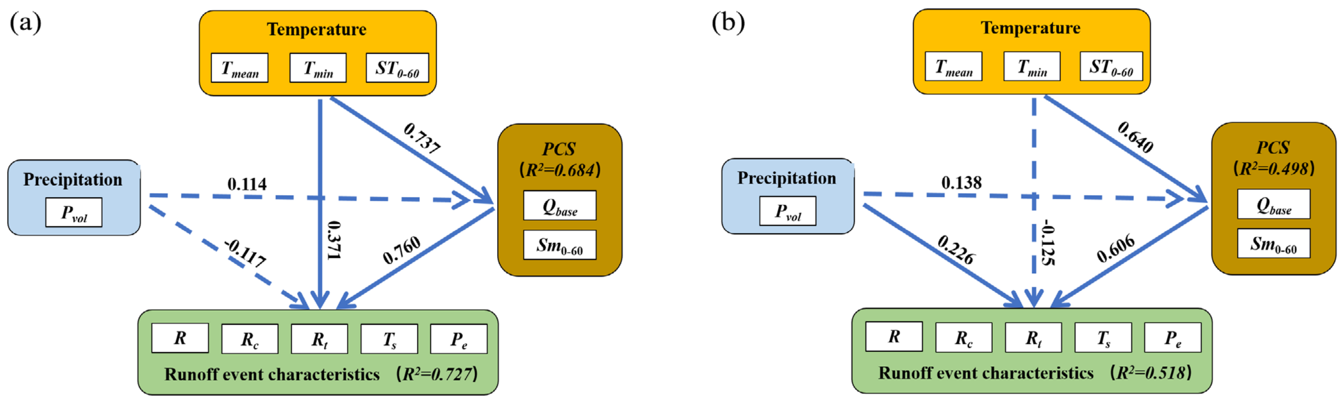

FIGURE 8 Structural equation models depicting direct and indirect drivers of runoff event characteristics and (a) single-peak model and (b) multiple-peak model. Solid arrows show significant effects and dashed arrows show non-significant effects. R^2 values indicate the percent of the variability in the dependent variables that the predictor variables explained. Comparative fit index (cfi) = 0.971 with single-peak model and 0.916 with multiple-peak model, compares the fit of the target model to an independent model with values over 0.9 indicating a good fit. Root-mean-square error of approximation (RMSEA) = 0.042 with single-peak model and 0.046 with multiple-peak model, estimates the error of approximation and thus relates to causal specification of model. A good model shows no significant difference between model and data.

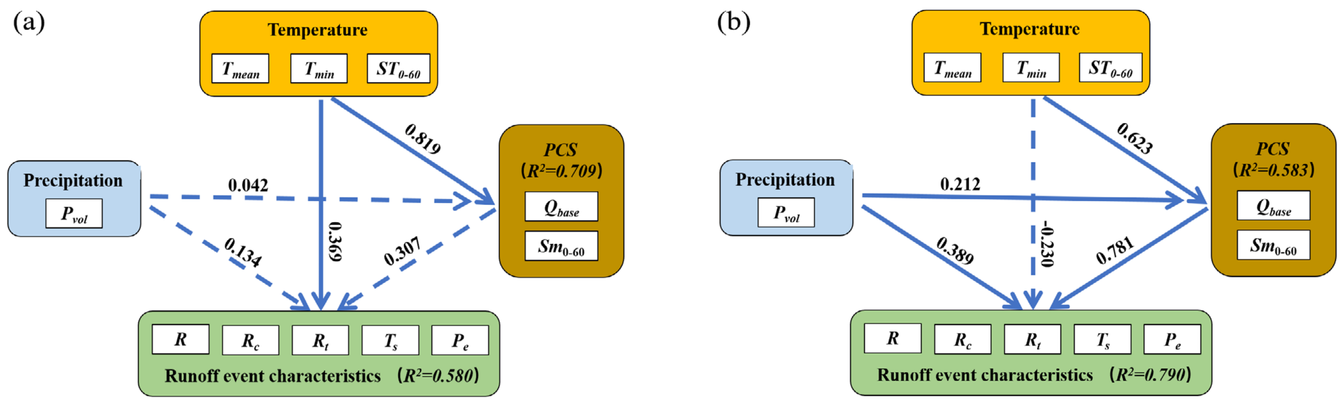

FIGURE 9 Structural equation models depicting direct and indirect drivers of runoff event characteristics and (a) soil melting period model and (b) stable period model. Solid arrows show significant effects and dashed arrows show no significant effects. Comparative fit index (cfi) = 0.905 with soil melting period model and 0.965 with stable period model. Root-mean-square error of approximation (RMSEA) = 0.052 with soil melting period model and 0.044 with stable period model.

to the catchment area having a high permeability. Event runoff coefficients exhibited strong seasonality. The catchment exhibited a gradual increase in event runoff coefficient with increasing pre-event baseflow and antecedent soil moisture, especially during stable period. The increasing trend in baseflow might be due to the increase in melting of the seasonally frozen soil within the watershed, which increased soil water storage capacity, forming more interflow, enhancing the regulation of aeration zone, and groundwater recharge. Furthermore, the increased melting caused infiltration during the thawing season, which increased baseflow. In addition, the formation of quick flow after rainfall was rapid, complicated, and variable owing to the steep topography. These findings were similar to those of Tarasova et al. (2018), who showed that mountainous catchments in Germany, with poor-developed soils, had a rapidly increasing event runoff coefficient as soil saturation rose, marking a clear transition between two functioning types. Event runoff generation through infiltration excess, as the result of intensive rainfall, seemed to be only possible in stable period, while heavy precipitation events were common during this period for the mountain catchments of the Qinghai-Tibet Plateau. Small precipitation events in the catchment dominated in the latter part of the soil melting period. However, the arrival of the plant growing season leads to increased transpirational water consumption, presence of seasonally frozen soil thaw, and the high permeability of mountain catchments in arid regions. This showed a hysteresis effect of runoff, characterized by high runoff coefficients in the stable period (Figure 10). It is characterized by high runoff coefficients for specified periods that do not increase as rainfall increases. Wang et al. (2009) showed that the runoff coefficients of streamflow were 0.6 from May to June in a permafrost watershed on the Qinghai-Tibet Plateau. Xiao et al. (2020) reported that the average runoff coefficients of runoff plots on the Plateau during the spring–summer transition period, from mid-May to early June, were relatively high at 1.7. The results of this study were consistent with the above-mentioned studies. The runoff coefficient of single-peak runoff events was the highest as 0.8, and the runoff coefficient of multiple-peak runoff events was 0.7, and both were distributed in August–November. This high runoff coefficient could be attributed to the controlling effects of frozen soil and meltwater from the cryosphere. The frozen soil acted as an impermeable layer, which promoted the runoff coefficient, and the meltwater from frozen soil provided an extra source of water for the generation of discharge. As permafrost thaws, soil moisture increases, which causes runoff thresholds to be reached quickly, causing high runoff coefficients.

5.2 | Process of runoff events generation and accumulation

For this catchment, higher storage capacity pre-event saturation (i.e., catchment saturation caused by a sequence of antecedent precipitation events) could be the main mechanism of event runoff generation (Coles & McDonnell, 2018), as it was unlikely that a single precipitation event would lead to catchment saturation. P_e and R_c show positive trends with changes in pre-event catchment state indicators (i.e., antecedent soil moisture, pre-event baseflow, and soil temperature), which are commonly observed phenomena in runoff events. In a single-peak event, light precipitation corresponds to a large runoff coefficient due to the existence of this recharge mechanism. As soil infiltration is greater in light precipitation events than in heavy precipitation events, infiltration would preferentially recharge underground storage, especially during precipitation periods. In this mountainous alpine catchment with poor-developed soils, the event runoff coefficient increased rapidly as soil saturation rose, marking a clear transition between two functioning types (Tarasova et al., 2018). A threshold-like dependence between event runoff coefficients and antecedent soil moisture, 0.20 m^3/m^3 in this article, could be an indicator of a critical switch in the catchment behaviour, to which the hydrologic connectivity and its characteristic pattern change corresponds (Graeff et al., 2012).

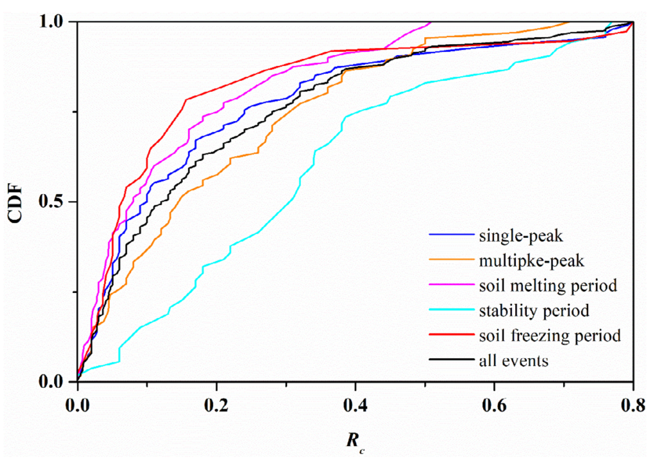

FIGURE 10 Cumulative distribution function (CDF) of event runoff coefficient

Threshold effects were widely observed in studies of hydrological responses in mountain catchments, and the thresholds varied with different properties, such as soil temperature, saturated hydraulic conductivity, soil porosity, and saturated soil moisture content (McMillan & Srinivasan, 2015; Scaife et al., 2020; Wei et al., 2020). Threshold effects were prevalent in runoff events of this study (Figure 5). As shown in Figure 5, the red dashed line indicates the threshold rainfall for single-peak events is 80 mm, with an average of 10.2 mm, while the multi-peak events were evenly distributed in the range of 0–137.0 mm, with an average of 36.1 mm. The antecedent soil moisture threshold of runoff events was greater than 0.1 m^3/m^3, and the soil temperatures threshold were greater than 0°C. The duration, from the beginning of the event until the day when peak discharge was observed, decreased gradually in single-peak events, normalized by the total duration of the event, with increasing soil temperature. It was dominated by single-peak runoff events of long-term, small event peak discharge when the pre -baseflow was less than 0.1 mm/day and the temperature was lower than 0°C.

5.3 | Drivers of runoff events

The four runoff event-scale SEM developed for a mountainous catchment in the arid region of the Qinghai-Tibet Plateau demonstrated linkages between precipitation, temperature, pre-event catchment state and runoff processes. The model illustrated that temperature had a stronger impact on the hydrological regime of mountain catchments in arid regions (Table 2). In the single-peak model, temperature affected runoff processes through direct effects on runoff processes and indirect effects on pre-event catchment state. In the multiple-peak model, temperature acted indirectly on runoff processes, mainly through direct effects on pre-event catchment state. A similar indirect temperature effect was observed in runoff generation processes from the spring–summer transition period to the summer months in a catchment on the Qinghai-Tibet Plateau by Xiao et al. (2020), who also developed SEM based on runoff generation processes.

This indicates that this study successfully constructed a structural equation model to predict the influencing factors of the runoff process at the scale of runoff events for a mountain catchment with seasonally frozen soil in the Qinghai-Tibet Plateau. The SEM only

TABLE 2 Standardized direct, indirect, and total effects of independent variables for the single-peak model, and multiple-peak model

	Single-peak model			Multiple-peak model		
Controlling variable	Direct	Indirect	Total	Direct	Indirect	Total
Temperature	0.371	0.560	0.931	−0.125	0.388	0.263
Precipitation	−0.117	0.086	−0.031	0.226	0.084	0.310
PCS	0.760	/	0.760	0.606	/	0.606

explained 50%–60% of runoff process, indicating the models could be improved, especially the multiple-peak model and stable period model. Two areas were suggested for possible model improvement for future research. Firstly, there may be incomplete and missing variables that were important to runoff processes. However, in the alpine mountain catchment of the Qinghai-Tibet Plateau, the soil layer was thin and widely distributed with seasonally frozen soil and permafrost. The above-ground and underground geological structures were complex and dynamic, such as the widespread distribution of weathered rubble and the frequent occurrence of preferential flow. There were many complexes, uncertain factors affecting the runoff process. The SEM required 5–10 samples per linkage in the model (Rosseel, 2012); however, this study was limited to 5 linkages for each model. Thus, not all variables that were important to the runoff generation process could be included. Secondly, improperly specified pathways and limitations in the data set may have caused insignificant linkages and the low explanation of variance in the SEM. Good linear relationships can be well represented in structural equation models; however, threshold effects present in this study suggest that some relationships may actually be nonlinear or discontinuous (Kreiling et al., 2020). Future modelling efforts incorporating nonlinear relationships may improve the predictive power of the models. Overall, the SEM represents an advanced approach which could improve our systematic understanding and prediction of runoff generation and convergence processes in the Qinghai-Tibet Plateau Mountain catchment.

6 | CONCLUSIONS

The study systematically analysed the runoff characteristics and the interactive effects of environmental factors and pre-event catchment state on the runoff process, based on the event runoff scale, in the mountainous catchment with a seasonally frozen soil distribution of the Qinghai-Tibet Plateau. This study found that the event runoff coefficient did not increase significantly with the increase of precipitation. Event runoff coefficients exhibited strong seasonality. The catchment exhibited a gradual increase in the event runoff coefficient with increasing pre-event baseflow and antecedent soil moisture, especially during stable period. Event runoff generation, through infiltration excess as the result of intensive rainfall, seemed to be only possible during the stable period, for which heavy precipitation events were common, for the mountain catchments of the Qinghai-Tibet Plateau. P_e and R_c showed positive trends with changes in pre-event catchment state indicators, which were commonly observed phenomena in runoff events. For this catchment, higher storage capacity pre-event saturation may be the main mechanism of event runoff generation, as was unlikely that a single precipitation event would lead to catchment saturation.

Four runoff event scale SEM developed for a mountainous catchment in the arid region of the Qinghai-Tibet Plateau demonstrated linkages between precipitation, temperature, pre-event catchment state and runoff processes. The model illustrated that in the single-peak model, temperature affected runoff processes through both direct effects on runoff processes and indirect effects on pre-event catchment state. In the multiple-peak model, temperature acted indirectly on runoff processes, mainly through direct effects on pre-event catchment state. Although there were still some suggestions for model improvement, structural equation models could explain more information about the effects of precipitation, temperature, and pre-event catchment state on hydrological regimes.

ACKNOWLEDGEMENTS

We are very grateful to the editor and anonymous referees for their valuable comments that have improved the manuscript. Furthermore, we would like to thank Editage (www.editage.cn) for English language editing.

FUNDING INFORMATION

This research has been supported by the National Natural Science Foundation of China (No. 41901044, 41901050, 41621001), and Foundation for Excellent Youth Scholars of Northwest Institute of Eco-Environment and Resources, Chinese Academy of Sciences (No. FEYS2019019). The Strategic Priority Research Program of the Chinese Academy of Sciences (CAS) (XDA23060301).

CONFLICT OF INTEREST

The contact author has declared that neither they nor their co-authors have any competing interests.

DATA AVAILABILITY STATEMENT

The data used in this study can be accessed by contacting the first author (linpengfei@lzb.ac.cn) and corresponding author (hzbmail@lzb.ac.cn) based on reasonable request.

ORCID

Pengfei Lin https://orcid.org/0000-0002-9798-8670
Xi Zhu https://orcid.org/0000-0001-9259-1490

REFERENCES

Chen, R. S., Song, Y. X., Kang, E. S., Han, C. T., Liu, J. F., Yang, Y., Qing, W. W., & Liu, Z. W. (2014). A cryosphere-hydrology observation system in a small alpine watershed in the Qilian Mountains of China and its meteorological gradient. *Arctic, Antarctic, and Alpine Research*, *46*, 505–523.

Cheng, G., Li, X., Zhao, W., Xu, Z., Feng, Q., Xiao, S., & Xiao, H. (2014). Integrated study of the water–ecosystem–economy in the Heihe River basin. *National Science Review*, *1*, 413–428.

Coles, A. E., & McDonnell, J. J. (2018). Fill and spill drives runoff connectivity over frozen ground. *Journal of Hydrology*, *558*, 115–128. https://doi.org/10.1016/j.jhydrol.2018.01.016

Edokpa, D., Milledge, D., Allott, T., Holden, J., Shuttleworth, E., Kay, M., Johnston, A., Millin-Chalabi, G., Scott-Campbell, M., & Chandler, D. (2022). Rainfall intensity and catchment size control storm runoff in a gullied blanket peatland. *Journal of Hydrology*, *127688*. https://doi.org/10.1016/j.jhydrol.2022.127688

Gao, H., Wang, J., Yang, Y., Pan, X., Ding, Y., & Duan, Z. (2021). Permafrost hydrology of the Qinghai-Tibet plateau: A review of processes and modeling. *Frontiers in Earth Science*, *535*. https://doi.org/10.3389/feart.2020.576838

Graeff, T., Zehe, E., Blume, T., Francke, T., & Schroder, B. (2012). Predicting event response in a nested catchment with generalized linear models and a distributed watershed model. *Hydrological Processes*, *26*, 3749–3769. https://doi.org/10.1002/hyp.8463

Han, L., & Menzel, L. (2022). Hydrological variability in southern Siberia and the role of permafrost degradation. *Journal of Hydrology*, *604*, 127203.

Huo, J., Liu, C., Yu, X., Chen, L., Zheng, W., Yang, Y., & Yin, C. (2021). Direct and indirect effects of rainfall and vegetation coverage on runoff, soil loss, and nutrient loss in a semi-humid climate. *Hydrological Processes*, *35*, e13985.

Ireson, A. M., van der Kamp, G., Ferguson, G., Nachshon, U., & Wheater, H. S. (2013). Hydrogeological processes in seasonally frozen northern latitudes: Understanding, gaps and challenges. *Hydrogeology Journal*, *21*, 53–66. https://doi.org/10.1007/s10040-012-0916-5

Jin, X.-Y., Jin, H.-J., Iwahana, G., Marchenko, S. S., Luo, D.-L., Li, X.-Y., & Liang, S.-H. (2021). Impacts of climate-induced permafrost degradation on vegetation: A review. *Advances in Climate Change Research*, *12*, 29–47.

Kirkby, M. (1988). Hillslope runoff processes and models. *Journal of Hydrology*, *100*, 315–339.

Koch, J. C., Kikuchi, C. P., Wickland, K. P., & Schuster, P. (2014). Runoff sources and flow paths in a partially burned, upland boreal catchment underlain by permafrost. *Water Resources Research*, *50*, 8141–8158.

Kreiling, R. M., Thoms, M. C., Bartsch, L. A., Larson, J. H., & Christensen, V. G. (2020). Land use effects on sediment nutrient processes in a heavily modified watershed using structural equation models. *Water Resources Research*, *56*. https://doi.org/10.1029/2019wr026655

Lafrenière, M. J., & Lamoureux, S. F. (2019). Effects of changing permafrost conditions on hydrological processes and fluvial fluxes. *Earth-Science Reviews*, *191*, 212–223.

Lin, L., Gao, M., Liu, J., Wang, J., Wang, S., Chen, X., & Liu, H. (2020). Understanding the effects of climate warming on streamflow and active groundwater storage in an alpine catchment: The upper Lhasa River. *Hydrology and Earth System Sciences*, *24*, 1145–1157.

Lin, P., He, Z., Du, J., Chen, L., & Jing, L. (2018). Impacts of climate change on reference evapotranspiration in the Qilian Mountains of China: Historical trends and projected changes. *International Journal of Climatology*, *38*, 2980–2993.

Lin, P., He, Z., Du, J., Chen, L., Zhu, X., & Tian, Q. (2020). Processes of runoff in seasonally-frozen ground about a forested catchment of semi-arid mountains. *Sciences in Cold and Arid Regions*, *12*, 272–283.

Lyne, V. D., & Hollick, M. (1979). *Stochastic time-variable rainfall-runoff modeling*. Aust. Natl. Conf. Publ.

Ma, R., Sun, Z., Hu, Y., Chang, Q., Wang, S., Xing, W., & Ge, M. (2017). Hydrological connectivity from glaciers to rivers in the Qinghai–Tibet plateau: Roles of suprapermafrost and subpermafrost groundwater. *Hydrology and Earth System Sciences*, *21*, 4803–4823.

McMillan, H. K., & Srinivasan, M. S. (2015). Characteristics and controls of variability in soil moisture and groundwater in a headwater catchment. *Hydrology and Earth System Sciences*, *19*, 1767–1786. https://doi.org/10.5194/hess-19-1767-2015

Mei, Y., & Anagnostou, E. N. (2015). A hydrograph separation method based on information from rainfall and runoff records. *Journal of Hydrology*, *523*, 636–649. https://doi.org/10.1016/j.jhydrol.2015.01.083

Qin, Y., Lei, H., Yang, D., Gao, B., Wang, Y., Cong, Z., & Fan, W. (2016). Long-term change in the depth of seasonally frozen ground and its ecohydrological impacts in the Qilian Mountains, northeastern Tibetan plateau. *Journal of Hydrology*, *542*, 204–221. https://doi.org/10.1016/j.jhydrol.2016.09.008

R Core Team. (2019). *R: A language and environment for statistical computing*. R Foundation for Statistical Computing. https://www.R-project.org/

Rey, D. M., Hinckley, E.-L. S., Walvoord, M. A., & Singha, K. (2021). Integrating observations and models to determine the effect of seasonally frozen ground on hydrologic partitioning in alpine hillslopes in the Colorado Rocky Mountains, USA. *Hydrological Processes*, *35*, e14374. https://doi.org/10.1002/hyp.14374

Rosseel, Y. (2012). lavaan: An R package for structural equation modeling. *Journal of Statistical Software*, *48*, 1–36. https://doi.org/10.18637/jss.v048.i02

Rushlow, C. R., & Godsey, S. E. (2017). Rainfall-runoff responses on Arctic hillslopes underlain by continuous permafrost, North Slope, Alaska, USA. *Hydrological Processes*, *31*, 4092–4106. https://doi.org/10.1002/hyp.11294

Scaife, C. I., Singh, N. K., Emanuel, R. E., Miniat, C. F., & Band, L. E. (2020). Non-linear quickflow response as indicators of runoff generation mechanisms. *Hydrological Processes*, *34*, 2949–2964. https://doi.org/10.1002/hyp.13780

Serrano-Notivoli, R., Martinez-Salvador, A., Garcia-Lorenzo, R., Espin-Sanchez, D., & Conesa-Garcia, C. (2022). Rainfall-runoff relationships at event scale in western Mediterranean ephemeral streams. *Hydrology and Earth System Sciences*, *26*, 1243–1260. https://doi.org/10.5194/hess-26-1243-2022

Shi, R., Yang, H., & Yang, D. (2020). Spatiotemporal variations in frozen ground and their impacts on hydrological components in the source region of the Yangtze River. *Journal of Hydrology*, *590*, 125237.

Smith, A., Tetzlaff, D., Laudon, H., Maneta, M., & Soulsby, C. (2019). Assessing the influence of soil freeze–thaw cycles on catchment water storage–flux–age interactions using a tracer-aided ecohydrological model. *Hydrology and Earth System Sciences*, *23*, 3319–3334.

Steelman, C. M., Endres, A. L., & Van der Kruk, J. (2010). Field observations of shallow freeze and thaw processes using high-frequency ground-penetrating radar. *Hydrological Processes*, *24*, 2022–2033.

Sun, F., Lyu, Y., Fu, B., & Hu, J. (2016). Hydrological services by mountain ecosystems in Qilian Mountain of China: A review. *Chinese Geographical Science*, *26*, 174–187.

Tarasova, L., Basso, S., Zink, M., & Merz, R. (2018). Exploring controls on rainfall-runoff events: 1. *Time Series-Based Event Separation and Temporal Dynamics of Event Runoff Response in Germany, Water Resources Research*, *54*, 7711–7732. https://doi.org/10.1029/2018wr022587

Teufel, B., & Sushama, L. (2019). Abrupt changes across the Arctic permafrost region endanger northern development. *Nature Climate Change*, *9*, 858–862.

Wang, G., Hu, H., & Li, T. (2009). The influence of freeze–thaw cycles of active soil layer on surface runoff in a permafrost watershed. *Journal of Hydrology*, *375*, 438–449.

Watanabe, K., & Osada, Y. (2011). Comparison of hydraulic conductivity in frozen saturated and unfrozen unsaturated soils. *Vadose Zone Journal*, *15*(vzj2015), 0154. https://doi.org/10.2136/vzj2015.11.0154

Wei, L., Qiu, Z., Zhou, G., Kinouchi, T., & Liu, Y. (2020). Stormflow threshold behaviour in a subtropical mountainous headwater catchment during forest recovery period. *Hydrological Processes*, *34*, 1728–1740.

Xiao, X., Zhang, F., Che, T., Shi, X., Zeng, C., & Wang, G. (2020). Changes in plot-scale runoff generation processes from the spring–summer transition period to the summer months in a permafrost-dominated catchment. *Journal of Hydrology*, *587*, 124966. https://doi.org/10.1016/j.jhydrol.2020.124966

Yang, J., He, Z., Du, J., Chen, L., Zhu, X., Lin, P., & Li, J. (2017). Soil water variability as a function of precipitation, temperature, and vegetation: A case study in the semiarid mountain region of China. *Environmental Earth Sciences*, *76*, 206.

SUPPORTING INFORMATION

Additional supporting information can be found online in the Supporting Information section at the end of this article.

How to cite this article: Lin, P., He, Z., Du, J., Chen, L., Zhu, X., & Tian, Q. (2022). Understanding the hydrological regime based on the runoff events in a mountainous catchment with seasonally frozen soil in the Qinghai-Tibet plateau. *Hydrological Processes*, *36*(10), e14716. https://doi.org/10.1002/hyp.14716

APPENDIX A

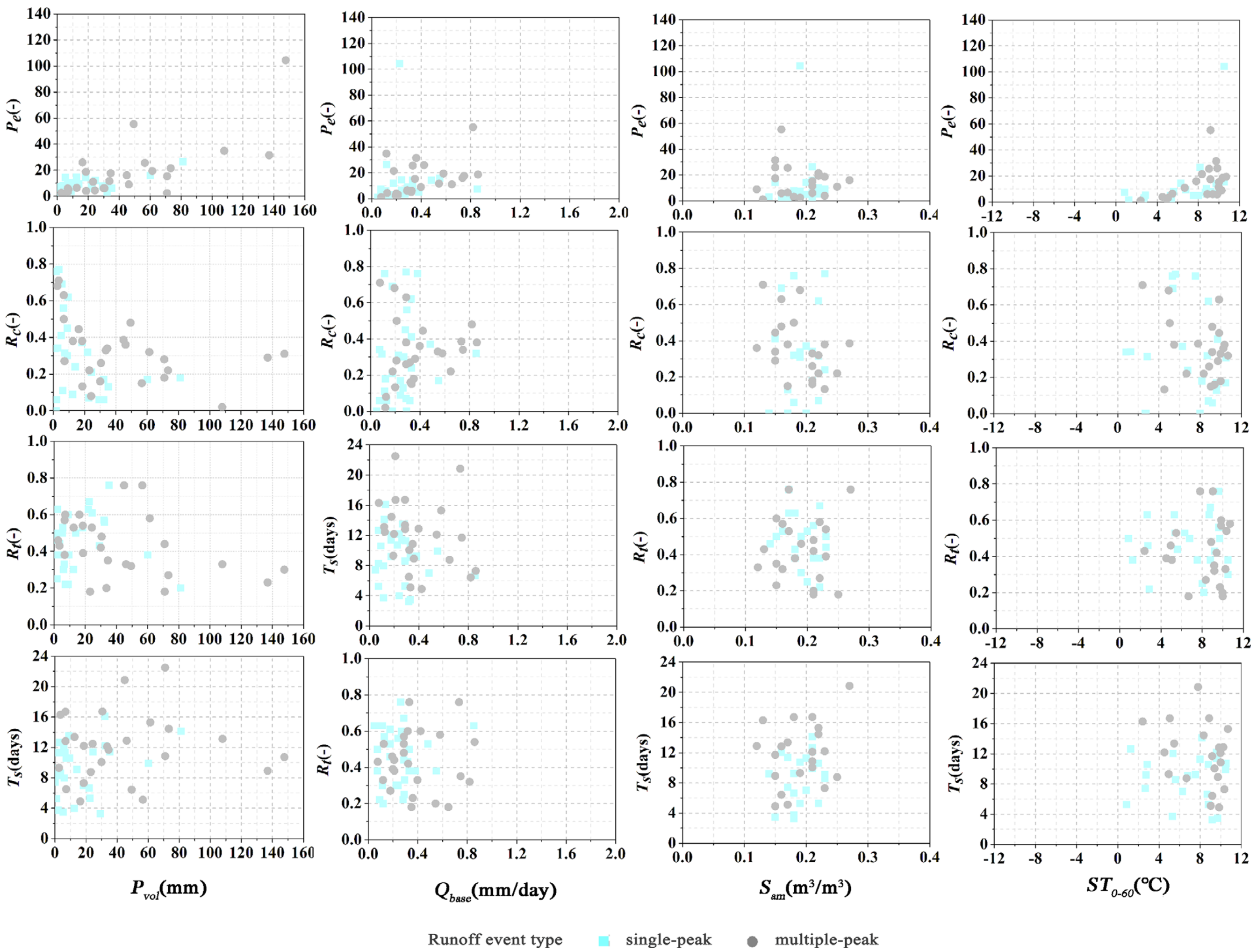

FIGURE A1 Seasonality of runoff event characteristics, stable period, August to November

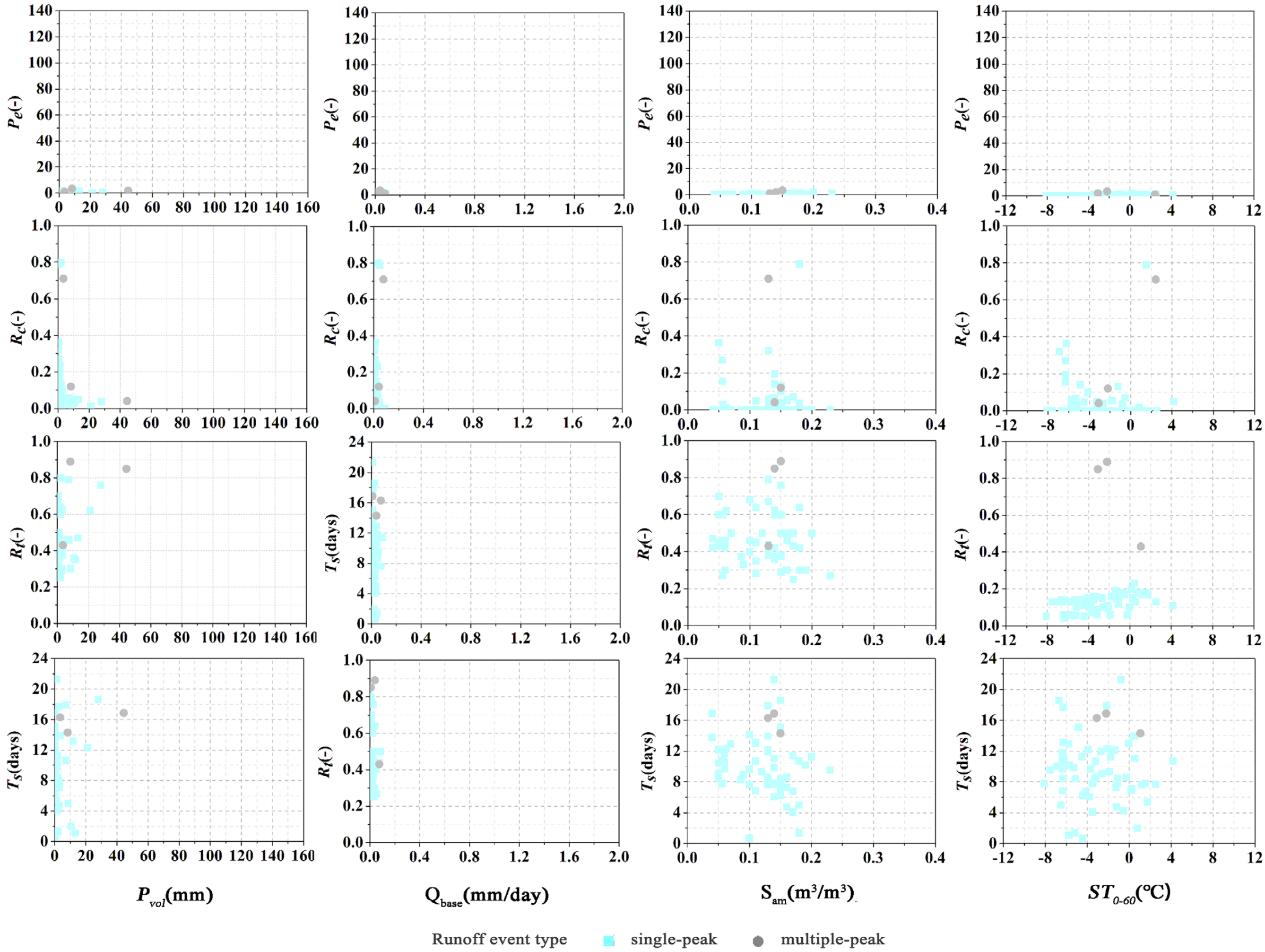

FIGURE A2 Seasonality of runoff event characteristics, soil freezing period, November to April